Fluid pressure penetration analysis of an O-ring seal of a pipe connection

This example demonstrates the use of fluid pressure penetration loads simulated as distributed surface loads or pairwise pressure loads. The demonstration is through an O-ring seal of a pipe connection.

The following Abaqus features are demonstrated:

- fluid pressure loads acting on a wetted surface region, with the wetted surface region evolving based on consideration of evolving contact conditions;
- self-contact of rubber after significant deformation; and
- use of explicit dynamic and implicit dynamic procedures to approximate quasi-static conditions (but with some dynamic effects remaining that require engineering judgment).

This page discusses:

Products: Abaqus/Standard Abaqus/Explicit

Application description

This example demonstrates fluid pressure-penetration loading in Abaqus for an O-ring seal simulation. O-rings are widely used in machine design to seal connections that require the transmission of fluid and gas. It is crucial for the design to ensure that the seal contains the fluid under operating conditions. The simulation tracks the evolution of the region exposed to fluid and applies surface pressure approximating the effects of fluid to that region without directly modeling the fluid. The purpose of this example is to provide perspective on modeling methods. Subsequent design iterations (not discussed in this example) might lead to significant design improvement.

Geometry

Figure 1 shows a schematic diagram for a scenario in which an O-ring helps seal a pipe connection. During installation, the O-ring is compressed into the seal groove in the lower flange to create a tight and leak-proof seal, as shown in the cut view of Figure 2.

A simplified model is employed that focuses on the interactions between the O-ring and its surrounding surfaces where contact and fluid pressure loads develop. The O-ring is relatively soft; therefore, the surrounding parts are modeled as rigid surfaces for the preliminary study summarized in this example. Figure 3 shows an axisymmetric model in swept view, including the deformable O-ring and rigid surfaces representing the flat upper flange and the bottom flange with a channel. Figure 4 shows the relevant dimensions. The O-ring has an inner diameter of 4 mm and an outer diameter of 8 mm. The seal groove has a depth of 6.1 mm and top and bottom widths of 8.2 mm and 6.6 mm, respectively. The center of the O-ring is 20 mm from the axis of revolution.

Abaqus modeling approaches and simulation techniques

Mesh design

The finite element model is created with first-order axisymmetric elements with reduced integration (CAX4R). Figure 3 shows the finite element mesh in swept view.

Materials

The O-ring material is modeled as neo-Hookean hyperelastic with $C_{10} = 1000$ MPa and $D_1 = 1 \times 10^{-5}$ MPa^{-1}; such that the initial shear modulus, $\mu_0 = 2\,C_{10}$, is 2000 MPa, and the initial bulk modulus, $K_0 = \frac{2}{D_1}$, is 2×10^5 MPa. The ratio $\frac{K_0}{\mu_0} = 100$ corresponds to the suggested upper limit for Abaqus/Explicit, as discussed in Compressibility in Abaqus/Explicit.

The actual density of rubber is approximately 2.24×10^{-9} tonne/mm^3; however, due to the modeling strategy discussed in Analysis steps, the density assigned to the O-ring material for this example is 0.01 tonne/mm^3.

Interactions

All of the models considered have general contact specified globally to resist penetrations, and they all enforce a friction coefficient of 0.1. Contact occurs between the O-ring and adjacent surfaces, and the interior surface of the O-ring experiences self-contact.

The extent and evolution of the active fluid pressure–penetration loading region depends on the evolution of the contact state.

- Test case variations that use the surface-based fluid pressure–penetration loading capability use the contact state from general contact.
- Test case variations using the pairwise fluid pressure–penetration loading capability can only use the contact state from contact pairs. Therefore, these test variations have contact pairs defined between the O-ring and the adjacent rigid surfaces in addition to general contact that is specified globally.

- General contact creates contact exclusions for interactions associated with contact pairs automatically (as discussed in Defining the General Contact Domain for Abaqus/Explicit and Defining the General Contact Domain for Abaqus/Standard), such that those interactions are processed only by contact pairs. However, self-contact involving the interior surface of the O-ring is processed with general contact.

Analysis steps

The surface representing the bottom flange is held fixed throughout the simulation. The upper flange is moved downward by 3.9 mm to push the O-ring into the seal groove in Step 1. Step 2 simulates the effects of pressurized fluid entering the modeled region from the top left, which applies pressure to the exposed portion of the O-ring. It is assumed that the fluid slowly leaks into the region of the O-ring such that quasi-static conditions are a reasonable approximation (unless the seal is about to fail). However, the fluid pressure load magnitude is suddenly set to 750 MPa at the beginning of the second step.

Dynamic procedure types are used for this example to maximize robustness, due to the inherent stabilization effects of inertia. Material densities and step times are tuned such that the kinetic energy remains small compared to the strain energy for both steps. The duration of Step 1 is 0.8 seconds, and the duration of Step 2 is 0.1 seconds. The specified material density is much higher than that of the actual material, as discussed in Materials.

Application of fluid pressure loading on the O-ring in Step 2 causes dynamic overshoot in the displacement response, which tends to predict a larger penetration distance of fluid than would occur without dynamic overshoot.

Simulations with the following procedure sequences are considered:

- Procedure sequence 1:
  - Step 1: Explicit dynamic
  - Step 2: Explicit dynamic
- Procedure sequence 2:
  - Step 1: Implicit dynamic
  - Step 2: Implicit dynamic
- Procedure sequence 3:
  - Step 1: Implicit dynamic
  - Step 2: Explicit dynamic (after import from Abaqus/Standard to Abaqus/Explicit; as discussed in Transferring Results between Abaqus/Explicit and Abaqus/Standard)

Procedure sequence 3 is included because the most efficient modeling strategy for some fluid pressure-penetration workflows is to simulate preloading with Abaqus/Standard followed by import to Abaqus/Explicit for fluid pressure–penetration loading. Procedure sequence 3 does not result in the most efficient approach for this example among the cases considered.

Simulations with the following fluid pressure loading options are considered (see Fluid Pressure Penetration Loads for a discussion of these options):

- Pressure penetration load type 1: Pressure penetration loads applied as a distributed surface load, and the local algorithm controls the evolution of the region exposed to fluid pressure (applicable to Abaqus/Standard and Abaqus/Explicit).
- Pressure penetration load type 2: Pressure penetration loads applied as a distributed surface load, and the wetting advance algorithm controls the evolution of the region exposed to fluid pressure (applicable to Abaqus/Explicit).
- Pressure penetration load type 3: Pressure penetration loads applied by the pairwise fluid pressure penetration loading capability (applicable to Abaqus/Standard).

For the local algorithm, fluid pressure (PPRESS) is applied on the load surface where the contact stress (CPRESS) is below a critical contact pressure, which requires judicious selection of the load surface.

For the wetting advance algorithm and the algorithm used by the pairwise fluid pressure–penetration loading capability, you must specify a node or node set on the surface initially exposed to fluid pressure. The wetted surface region expands from these nodes when conditions are met for the fluid to penetrate into the contact interface.

Solution controls

In addition to using an artificially high material density, variable mass scaling is specified for Abaqus/Explicit steps to avoid having the stable time increment drop below a specified value. The first step causes significant distortion of some elements near the inner surface of the O-ring. Variable mass scaling adds a small amount of mass at these isolated locations to maintain the specified time increment size.

Discussion of results and comparison of cases

Simulation results for each model considered predict that the O-ring prevents leakage of fluid past the seal for the conditions described. A contour plot of the output variable PPRESS at a particular output frame shows the magnitude of the fluid pressure loading as a function of surface position. Animations and contour plots of PPRESS plots in Figure 5 through Figure 10 show the evolution of the fluid pressure loading on the O-ring and the deformation response for simulations associated with different model variations. Wetting is reversible for pressure-penetration load type 1 but irreversible for pressure-penetration load types 2 and 3. This distinction is apparent in the respective animations: the extent of the nonzero PPRESS region only grows for simulations with pressure-penetration load types 2 and 3, but it shrinks near the end of simulations with pressure-penetration load type 1.

History plots of kinetic energy (ALLKE) and internal energy (ALLIE) for Abaqus/Explicit and Abaqus/Standard simulations are shown in Figure 11 and Figure 12, respectively. The fluid pressure–penetration loading is applied in Step 2, which starts at simulation time 0.8. ALLKE remains a small fraction of ALLIE after ALLIE becomes significant; however, significant dynamic overshoot (and rebound) effects are apparent in the evolution of configurations in animations of Figure 5 through Figure 8. The maximum penetration distance of the fluid pressure into the contact interface for a truly static response would be less than what occurs for the simulations shown.

Performance

The model variations include three ways to simulate the first step (prior to fluid pressure–penetration loading) and six ways to simulate the second step. Abaqus/Explicit is fastest for the first step. Run times for the other cases and other steps relative to the run time of the first step in Abaqus/Explicit are as follows:

- The run time for the first step in Abaqus/Standard with general contact is 2.3 times longer than the run time in Abaqus/Explicit for the first step.
- The run time for the first step in Abaqus/Standard with general contact plus contact pairs is 2.1 times longer than the simulation in Abaqus/Explicit for the first step.
- The run time for the second step of non-import simulations in Abaqus/Explicit with either the local or the wetting advance algorithm is 15% percent of the run time in Abaqus/Explicit for the first step.
- The run time for the second step of import simulations in Abaqus/Explicit with either the local or the wetting advance algorithm is 17% percent of the run time in Abaqus/Explicit for the first step.
- The run time for the second step in Abaqus/Standard with the local algorithm is 5.4 times longer than the run time of the first step in Abaqus/Explicit.
- The run time for the second step in Abaqus/Standard with pairwise pressure penetration loading is 5.2 times longer than the run time of the first step in Abaqus/Explicit.

Import

Abaqus/Explicit is faster in both steps of this analysis. Results obtained with simulation sequence 3 (involving import to Abaqus/Explicit) are in good agreement with other results. Refer to Figure 13 through Figure 14 for a comparison of the fluid pressure (PPRESS) between simulation sequence 2 and 3.

Other considerations

The pressure penetration load applied at any increment is based on the contact status at the beginning of that increment. This can lead to dependence on the time increment size for Abaqus/Standard simulations with fluid pressure penetration. Small time increments are recommended to obtain accurate results. Abaqus/Explicit is well suited to treating complex evolutions like this due to its inherently small time increment sizes. For more information, see Fluid Pressure Penetration Loads. Based on the consistency of the Abaqus/Standard and Abaqus/Explicit results for this example, it appears that the time increment size Abaqus/Standard uses is adequately small in these simulations.

The use of nonphysical density in this example is based on the assumption that fluid slowly leaks into the region of the O-ring. A dynamic study with realistic density is required to investigate the effects of the sudden exposure of the O-ring to high pressure fluid.

Input files

O-ring_Thick_local_xpl.inp

Input file for procedure sequence 1 and pressure penetration load type 1.

O-ring_Thick_wetadv_xpl.inp

Input file for procedure sequence 1 and pressure penetration load type 2.

O-ring_Thick_local_std.inp

Input file for procedure sequence 2 and pressure penetration load type 1.

O-ring_Thick_cp_std.inp

Input file for procedure sequence 2 and pressure penetration load type 3.

O-ring_Thick_local_xpl_import.inp

Input file for Step 2 of procedure sequence 3 with pressure penetration load type 1 (importing from the end of Step 1 of O-ring_Thick_local_std.inp).

O-ring_Thick_wetadv_xpl_import.inp

Input file for Step 2 of procedure sequence 3 with pressure penetration load type 2 (importing from the end of Step 1 of O-ring_Thick_local_std.inp).

Figures

Figure 1. Schematic diagram for a pipe connection.

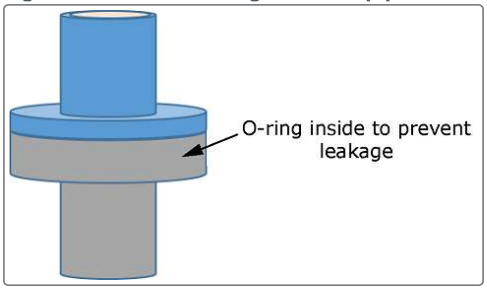

Figure 2. Cut view of the pipe connection.

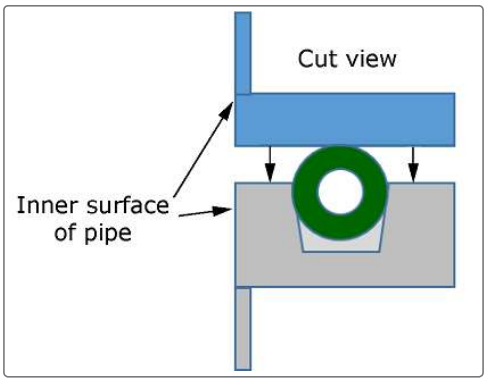

Figure 3. Axisymmetric model of the O-ring seal shown in swept view.

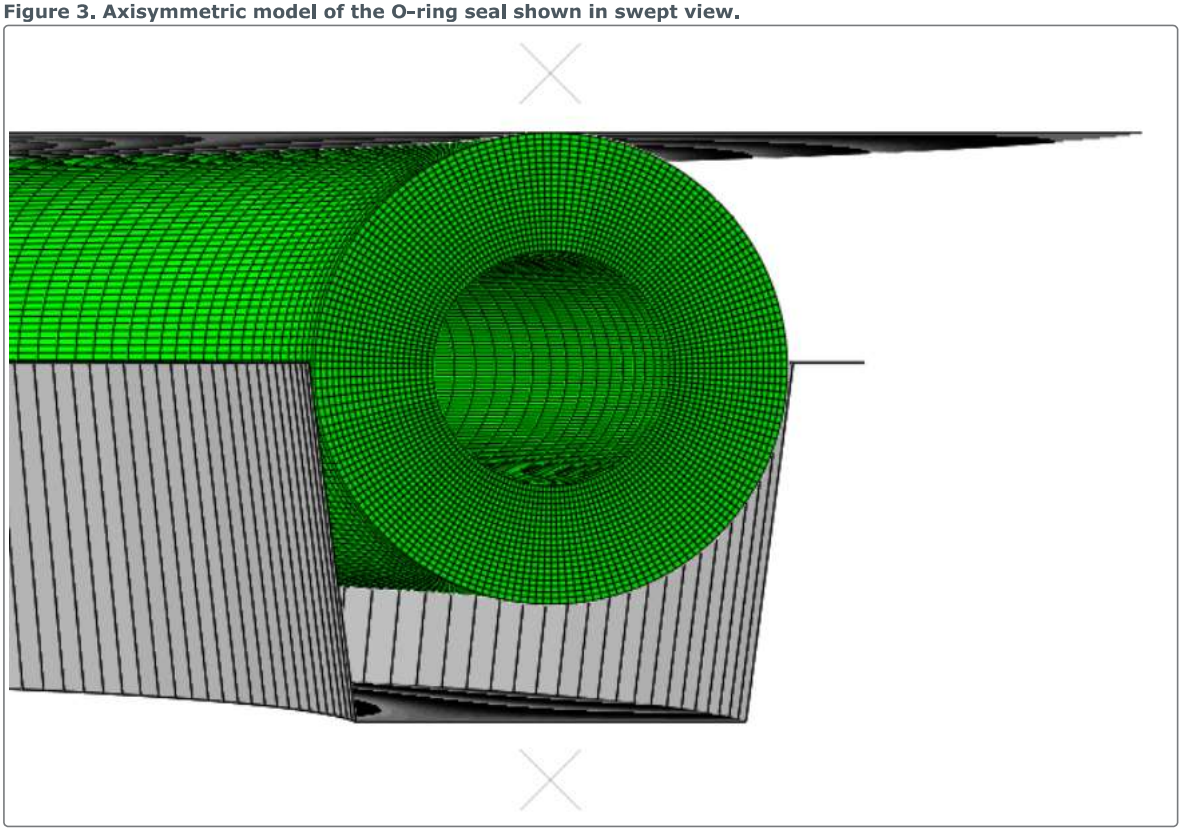

Figure 4. Dimensions of the O-ring seal.

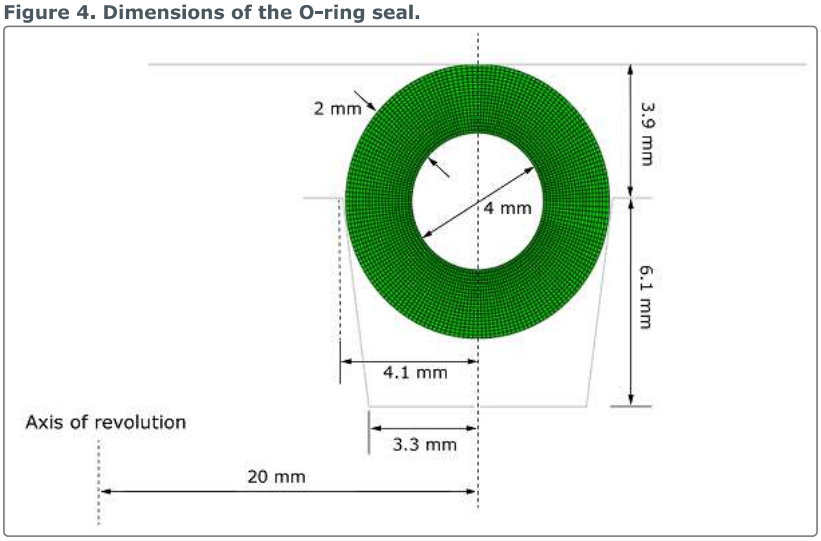

Figure 5. Evolution of fluid pressure PPRESS for procedure sequence 1 with pressure penetration load type 1.

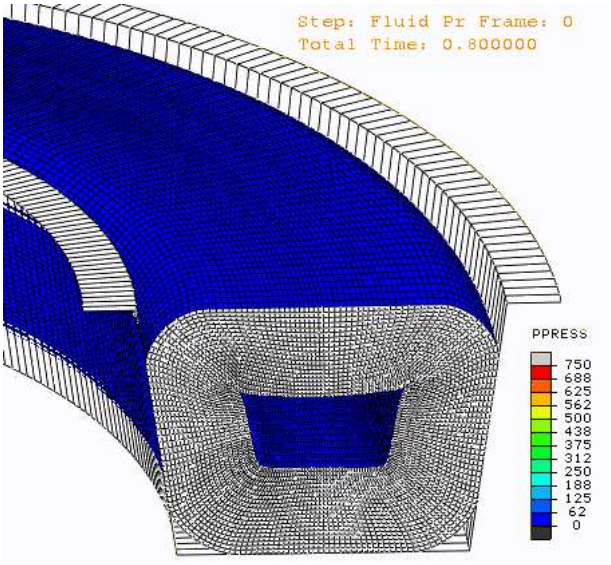

Figure 6. Evolution of fluid pressure PPRESS for procedure sequence 1 with pressure penetration load type 2.

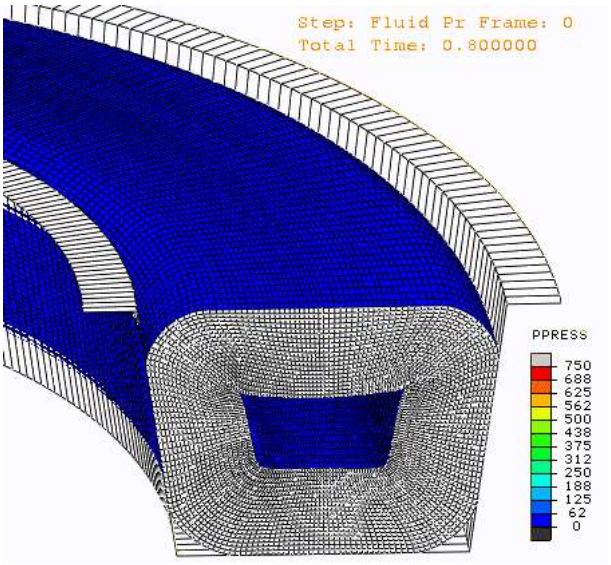

Figure 7. Evolution of fluid pressure PPRESS for procedure sequence 2 with pressure penetration load type 1.

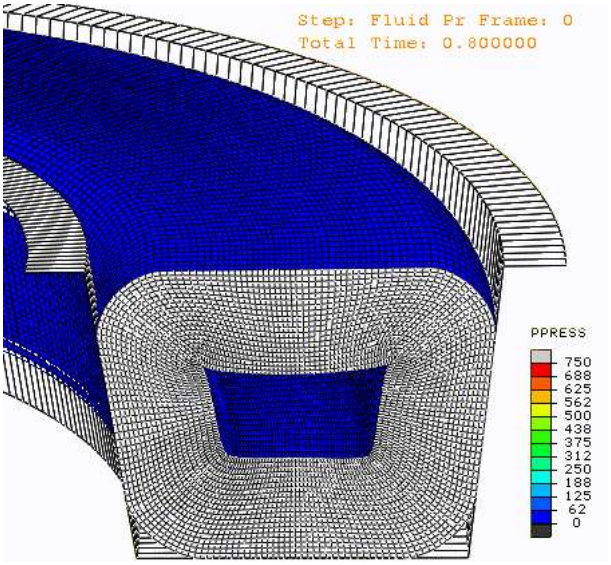

Figure 8. Evolution of fluid pressure PPRESS for procedure sequence 2 with pressure penetration load type 3.

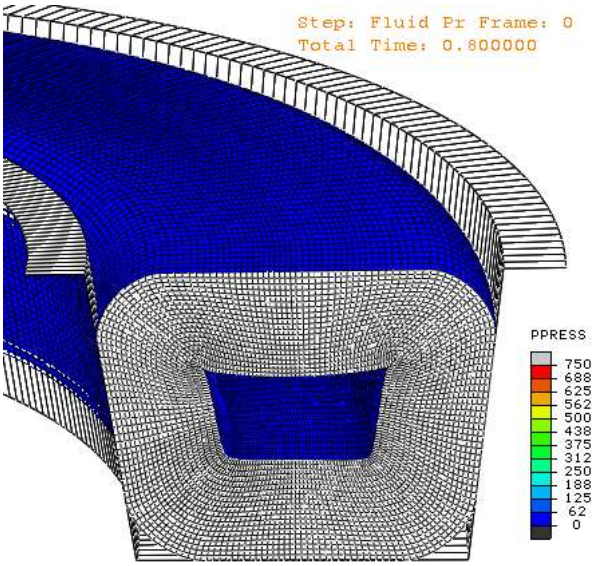

Figure 9. Fluid pressure PPRESS at the end of Step 2 for procedure sequence 1 with pressure penetration load type 1 (left) and 2 (right).

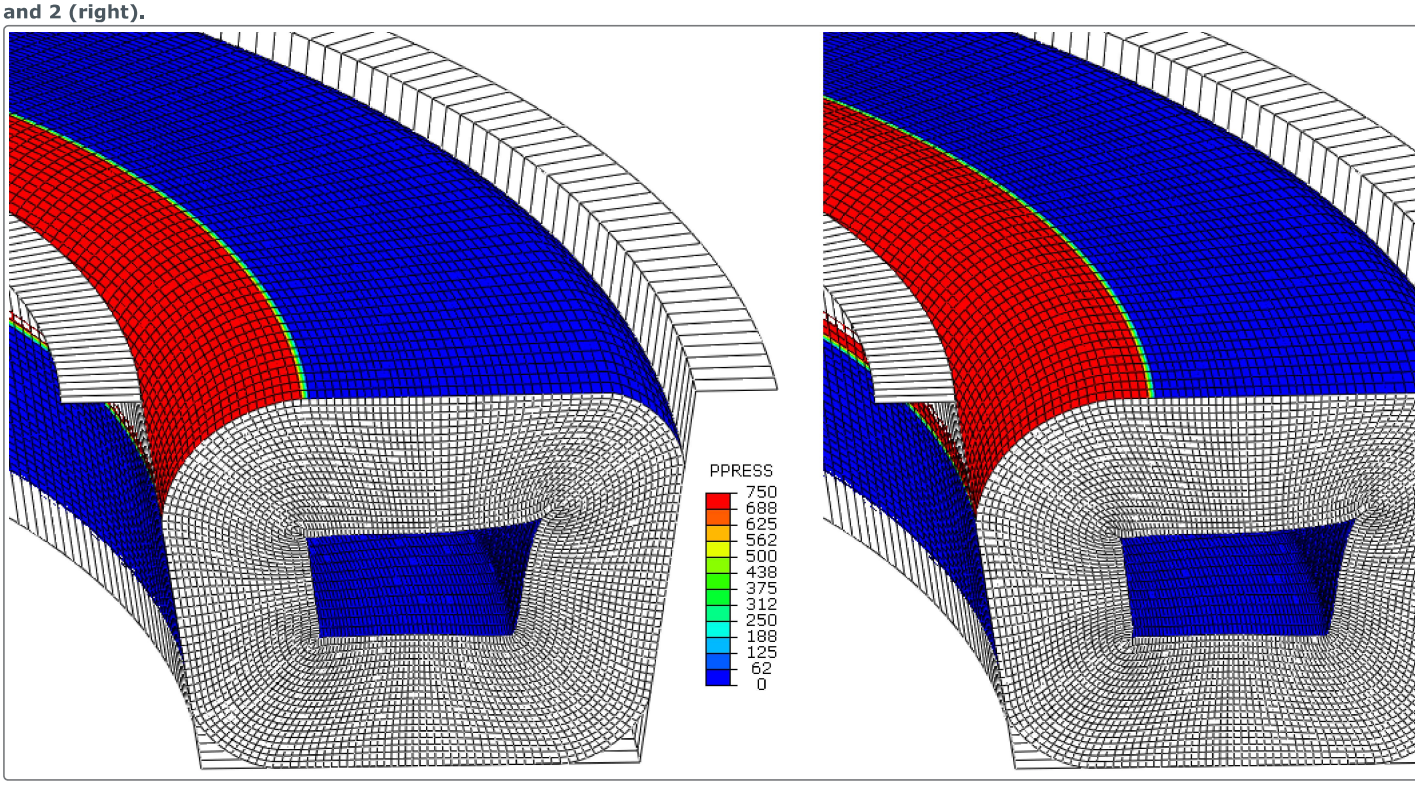

Figure 10. Fluid pressure PPRESS at the end of Step 2 for procedure sequence 2 with pressure penetration load type 1 (left) and 3 (right).

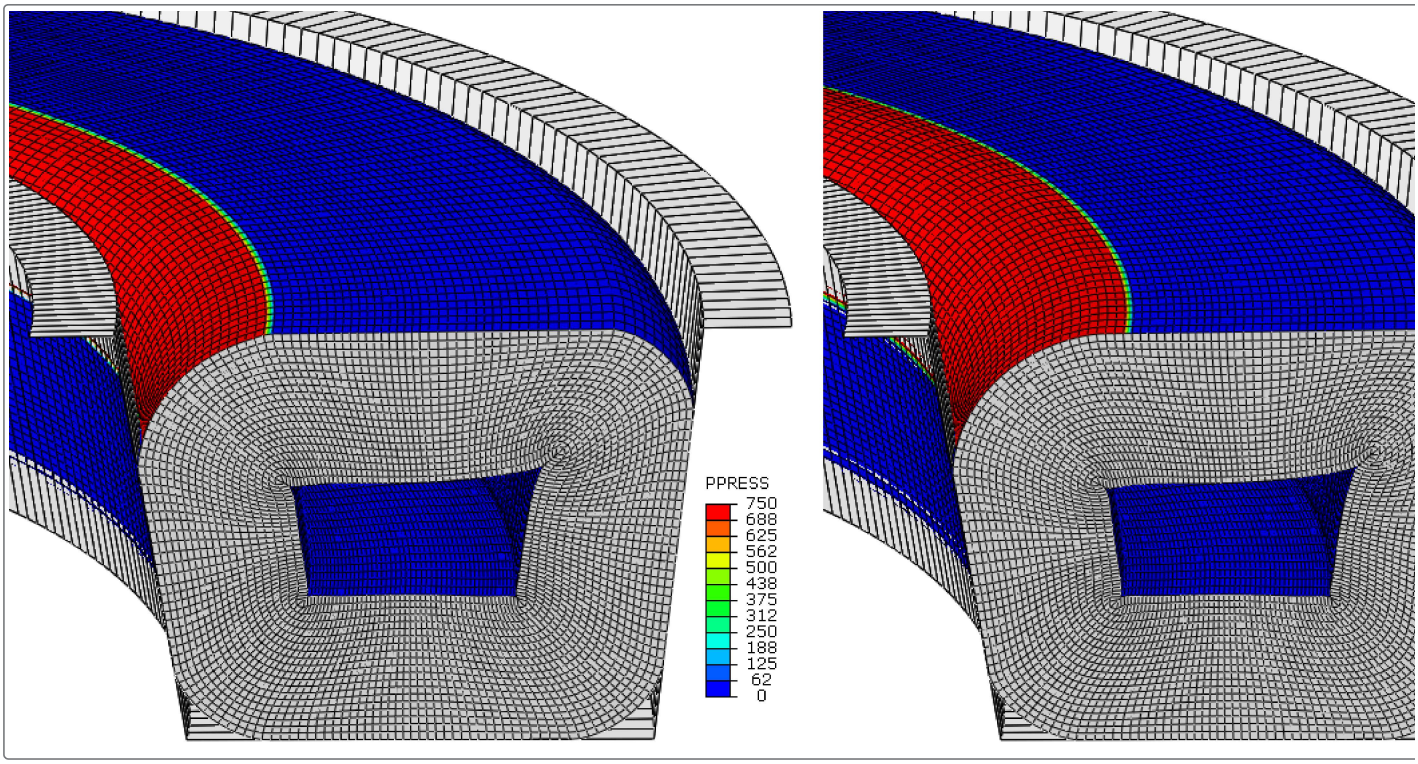

Figure 11. Kinematic energy (ALLKE) and Internal energy (ALLIE) history outputs for procedure sequence 1.

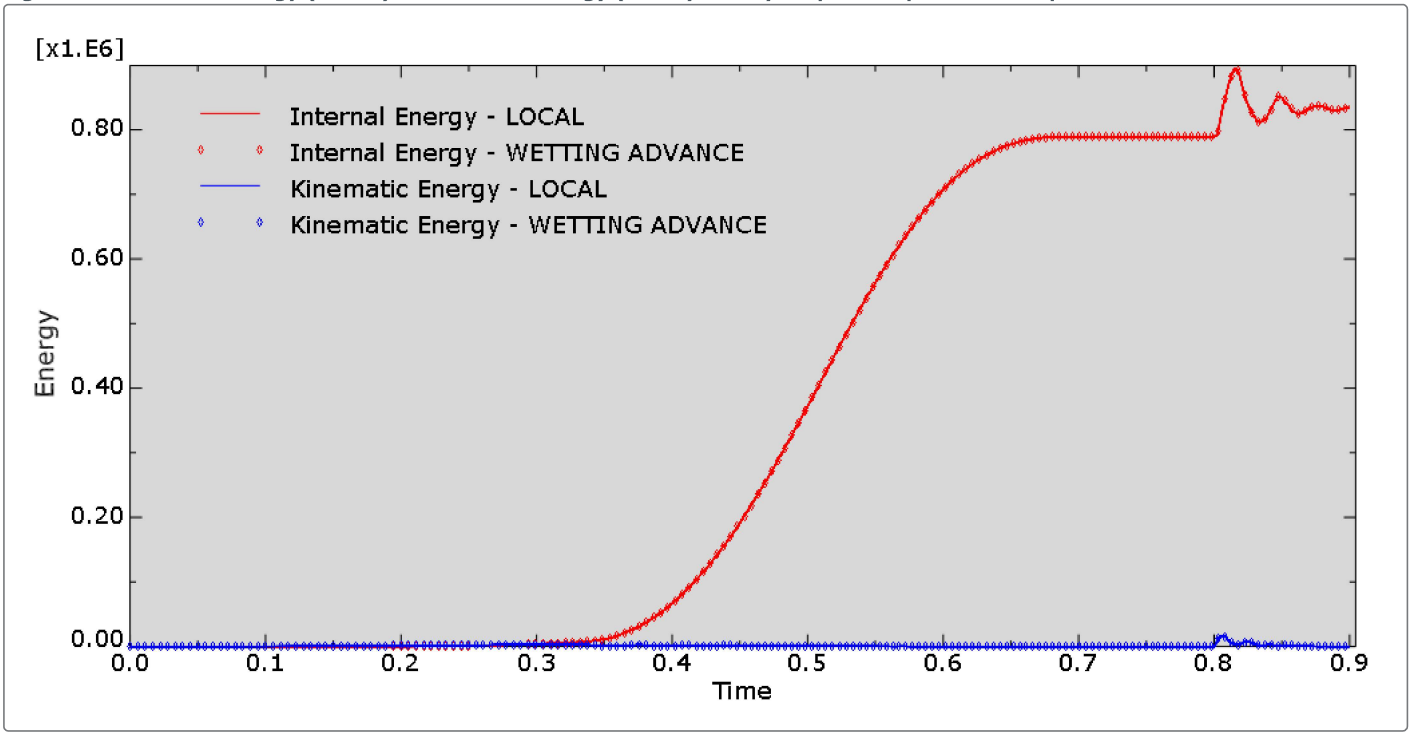

Figure 12. Kinematic energy (ALLKE) and Internal energy (ALLIE) history outputs for procedure sequence 2.

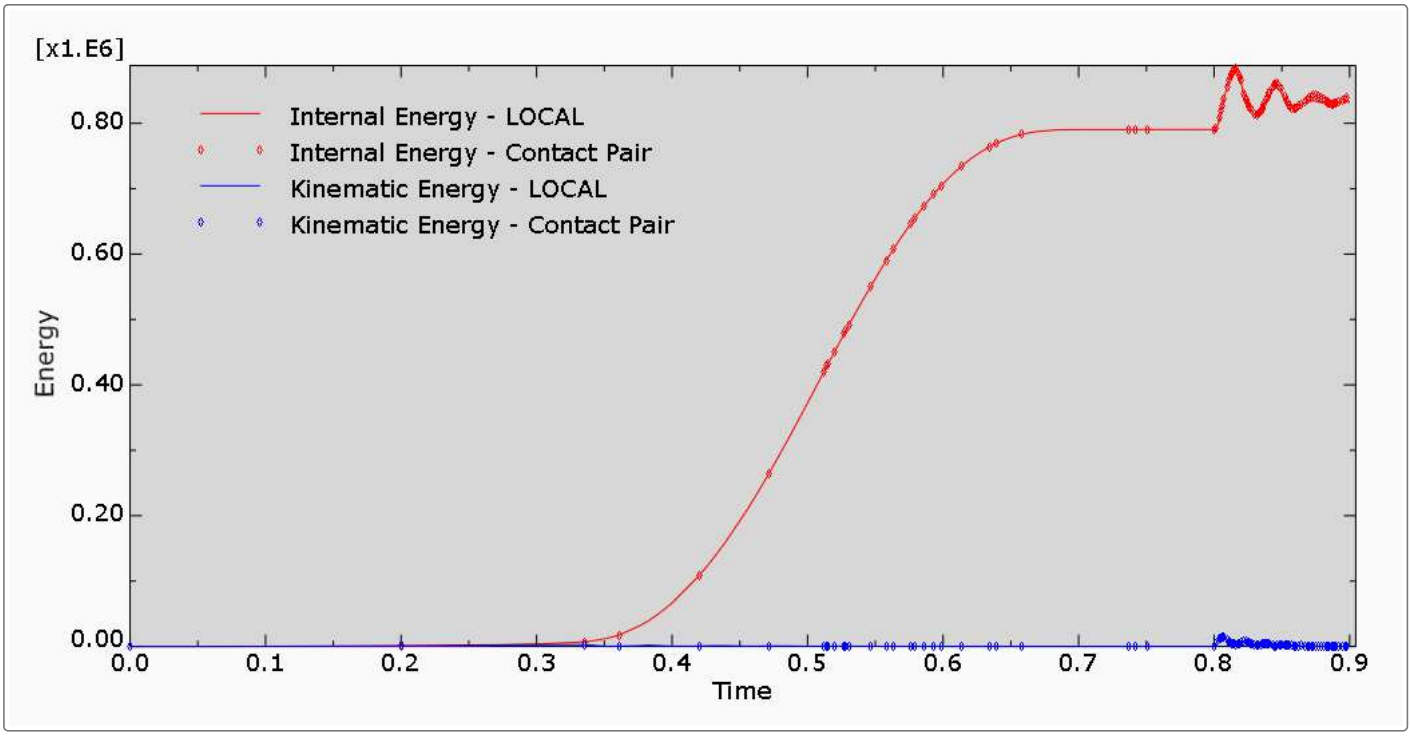

Figure 13. Fluid pressure PPRESS at the end of Step 2 for procedure sequence 1 (left) and 3 (right) with pressure penetration load type 1.

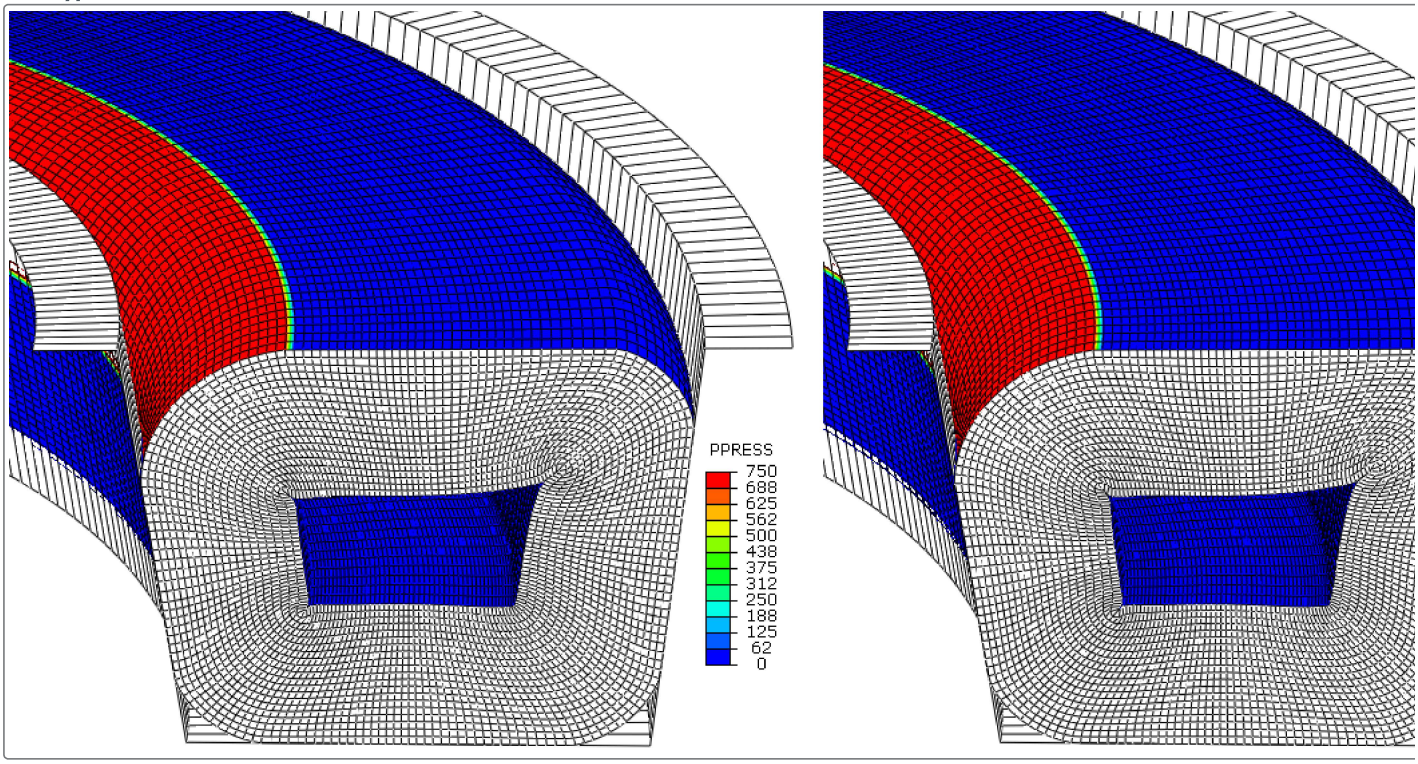

Figure 14. Fluid pressure PPRESS at the end of Step 2 for procedure sequence 1 (left) and 3 (right) with pressure penetration load type 2.

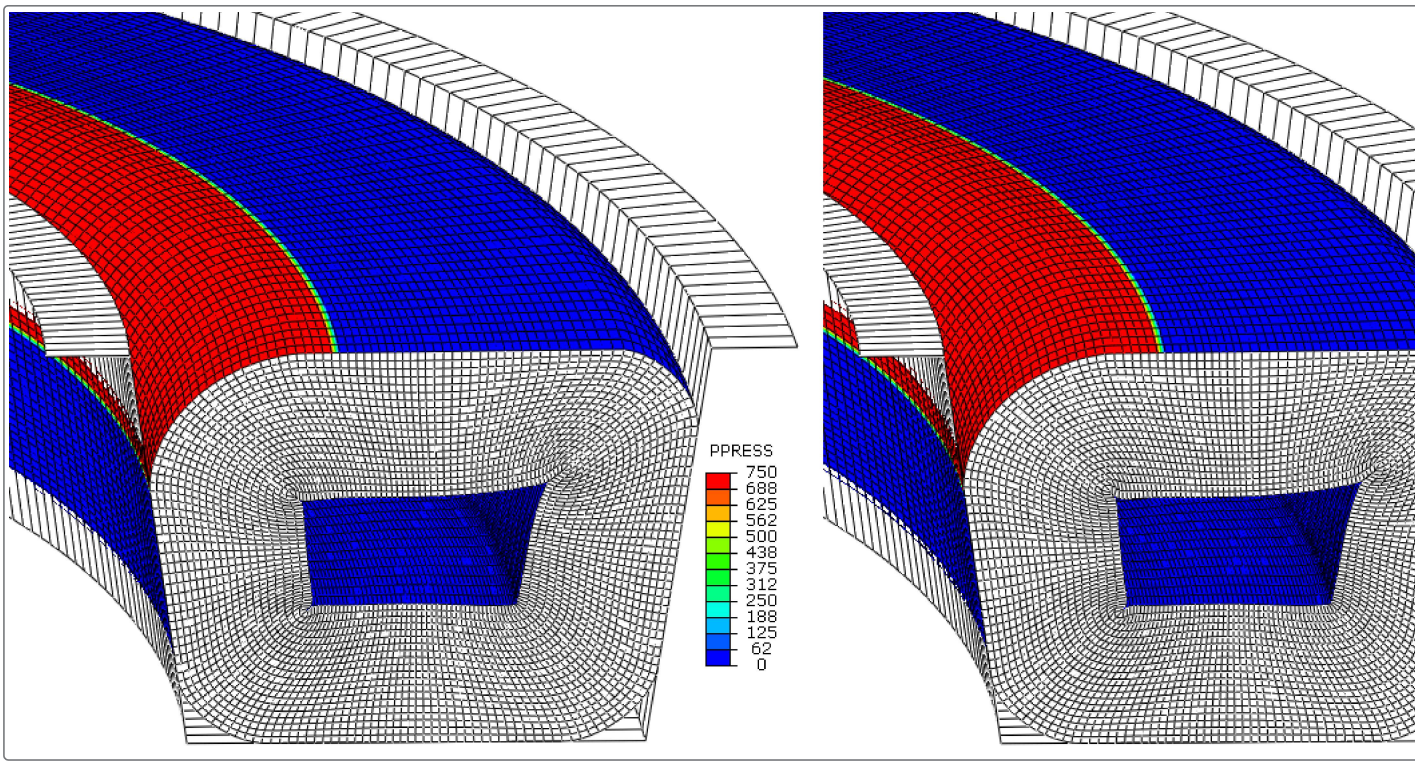
PPRESS
750
688
625
562
500
438
375
312
250
188
125
62
0